J. COMBIN. MATH. COMBIN. COMPUT. 127b (2025) 8139--8153

Journal of Combinatorial Mathematics
and Combinatorial Computing
www.combinatorialpress.com/jcmcc

Eco-environmental landscape characterization data based on artificial intelligence and neural network algorithms

Yuanke Zhang[1], Guangwei Wang[2,✉]

[1] School of Civil Engineering, Architecture and Environment, Hubei University of Technology, Wuhan, Hubei, 430000, China
[2] Aviation Service and Tourism Management College, Guilin University of Aerospace Technology, Guilin, Guangxi, 541004, China

ABSTRACT
In this study, the ecological environment landscape pattern index was selected to construct the ecological environment landscape data representation model under the self-organized feature mapping network (SOM) technique. The input data to the model were monitored under unsupervised conditions and made more sensitive to specific characterization information in the neuronal structure (Hebb), which resulted in different groups of regular data. The moving window method shows that the landscape index is unstable under the 1000-3000m window and the magnitude of change begins to decrease at the 4000m scale. The data tends to stabilize at 5000m scale, and the stability of the data decreases at 6000-7000m, and the anomalous data increases at this time. In terms of landscape level, the aggregation and connectivity of the overall landscape of the study area increased and landscape fragmentation, complexity and diversity decreased under the 4000m window. The land use change model based on SOM network can well reflect the law of land use change in the sample area, which greatly expands the spatial analysis research method of land use change.

Keywords: ecological environment landscape representation, landscape pattern index, self-organized feature mapping network, neuronal structure

1. Introduction

The ecological environment, as the basic condition for the survival of organisms, is an important place for the maintenance of biodiversity. Biodiversity is an important component of the earth's ecosystem and contributes to the balance and stability of the ecosystem [1-2]. When the ecological environment is damaged, it will lead to the loss of biological habitats and the decrease of biological populations, thus affecting the balance of the whole ecosystem. With the rapid development of science and

✉ Corresponding author.
E-mail address: wangguangwei198809@guat.edu.cn (G. Wang).
Received 20 February 2024; Revised 10 April 2024; Accepted 25 November 2024; Published Online 16 April 2025.
DOI: 10.61091/jcmcc127b-444

technology, artificial intelligence technology is more and more widely used in various fields, one of which is ecological environment monitoring [3-6].

Artificial intelligence technology can collect and monitor data in the ecological environment in real time through the combination of sensors and data processing systems. For example, air quality monitoring can be performed over large areas by utilizing high-resolution cameras carried by drones [7-10]. Artificial intelligence algorithms can automatically analyze the images to identify and calculate the concentrations of various pollutants in the air. In addition, AI can monitor noise and vibration levels in real time by setting up sensors. The application of these technologies makes the data collection for environmental monitoring more comprehensive and accurate [11-14]. In addition to collecting data from the environment, AI technology has an important role in environmental data analysis, environmental governance, and environmental safety [15-16]. The application of AI technology in ecological environment monitoring brings us a lot of convenience and importance, improves the precision of collecting and analyzing environmental data, and provides a more scientific and effective means for environmental governance and safety [17-19]. However, the ensuing challenge is how to ensure the reliability and safety of AI technology to avoid the adverse consequences due to wrong judgment and operation [20-21].

In this paper, the mechanism of self-organizing feature mapping neural network is given, by learning the features and topology inherent in the input vectors, the topological features are made visible on the output layer. And the process of characterization of this biological mechanism is realized by finding out meaningful laws from the input ecological landscape data in an unsupervised manner, Hebb neuron structure and unsupervised competitive learning rules are introduced. The training process of the neural network is proposed by calculating the degree of similarity between the comparison neurons and weight vectors so as to decide the best neuron that wins until the training is completed. Finally, in through the moving window method, the ecological landscape index of the study area is calculated, and this model is used to characterize the landscape pattern change of the ecological environment.

2. Ecological landscape characterization based on self-organized feature mapping network

2.1. *Analysis of ecological landscape pattern indices*

The landscape pattern index directly reflects the ecological status of landscape patches of each land use type, in order to evaluate the ecological landscape pattern more rationally and comprehensively. The formula and meaning of landscape pattern index are shown below. At the landscape level: landscape shape index (SHAPE-AM), area-weighted average patch subdimension (FRAC-AM), landscape spread index (CONTAG), cohesion index (COHESION), Shannon's diversity index (SHDI), and Shannon's homogeneity index (SHEI) are preferred; at the patch level: patch area (AREA-MN) is selected, number of patches (DP), edge density (ED), landscape shape index (SHAPE-AM), landscape cohesion index (Cohesion) and landscape aggregation index (AI). The ecological status of the landscape pattern and its evolution were analyzed and evaluated by analyzing the changes in the landscape pattern indices of land use types.

Number of patches (DP):

$$DP = N \tag{1}$$

N refers to the total number of ecological landscape patches, and the larger the value of DP indicates the greater the number of landscape patches in the ecosystem. If the total area of landscape patches remains constant, DP (number of patches) size can reflect DP (patch density) and the average landscape patch area size.

Edge Density (ED):

$$ED = \frac{\max(a_{ij})}{A} \times 100 \tag{2}$$

a_{ij} refers to the area of a particular landscape patch, and A refers to the proportion of the largest landscape patch of all landscapes in the ecosystem to the total area of the overall ecological landscape system. Its total area, the unit is km^2. ED refers to the value between [0, 100], the smaller the ED value, the smaller the area of the largest landscape patch in the land use landscape type; vice versa, the larger the area of the largest patch in the land use landscape type.

Landscape shape index (SHAPE-AM):

$$SHAPE\_AM = \frac{E}{\min E} \tag{3}$$

The Landscape Shape Index ($SHAPE\_AM$) is commonly used as a measure of landscape patch shape variation, with larger values of LSI indicating greater irregularity of the landscape type. The degree of fragmentation of regional habitat patches is associated with the stronger the degree of disturbance by whiteland and perceived disturbance.

Area-weighted semi-average patch dimensioning (FRAC_AM):

$$FRAC\_AM = \frac{2}{\dfrac{[N\sum_{i=1}^{n}\sum_{j=1}^{n}(\ln p_{ij} \ln a_{ij})] - [(\sum_{i=1}^{m}\sum_{j=1}^{n}\ln p_{ij}) - (\sum_{i=1}^{m}\sum_{j=1}^{n}\ln a_{ij})]}{(N\sum_{i=1}^{m}\sum_{j=1}^{n}\ln p_{ij}^{2}) - (\sum_{i=1}^{m}\sum_{j=1}^{n}\ln p_{ij})}} \tag{4}$$

The area-weighted average patch dimension $(FRAC\_MN)$ is often used to measure the redundancy of the landscape shape of habitat patches, taking a value between [1, 1. 6], the smaller the value of $FRAC\_MN$ and the closer the value to 1, the more the shape of the landscape patch approximates a rectangular shape, and the disturbance of the landscape caused by the natural or anthropogenic activity disturbance is also relatively large.

Landscape Spreading Degree Index (CONTAG):

$$CONTAG = [1 + \frac{\sum_{i=1}^{m}\sum_{k=1}^{m}[p_i \frac{g_{ik}}{\sum_{k=1}^{m} g_{ik}}][\ln(p_i \frac{g_{ik}}{\sum_{k=1}^{m} g_{ik}})]}{2\ln(m)}] \times 100 \tag{5}$$

Spreading index $(CONTAG)$ is often used to reflect the spreading and expansion trend of landscape patches with spatial distribution differences. The smaller the value of $CONTAG$, the more small patches exist within the landscape type, which intuitively reflects the strong degree of fragmentation of the landscape patch, and vice versa, which indicates that the landscape patch has strong internal connectivity.

Cohesion index (COHESION):

$$COHESION = [1 - \frac{\sum_{j=1}^{m} p_{ij}}{\sum_{j=1}^{m} p_{ij}\sqrt{a_{ij}}}][1 - \frac{1}{\sqrt{A}}]^{-1} \times 100 \tag{6}$$

The cohesion index $(COHESION)$ reflects the degree of cohesion of the patches, a_{ij} refers to the area (m^2) of the j th patch in the landscape category i; p_{ij} represents the perimeter (m) of the j th patch in the landscape category i, and A is the total area of the landscape (hm^2). The magnitude of the value reflects the degree of connectivity of natural landscapes.

Shannon Diversity Index (SHDI):

$$SHDI = -\sum_{i=1}^{m}(p_i \ln p_i) \tag{7}$$

The Shannon diversity index ($SHDI$) is commonly used to measure the spatial heterogeneity of ecological landscapes. When its $SHDI$ is 0, it indicates that there is only 1 overall landscape patch type, and the larger $SHDI$ is, it indicates that there are multiple types of landscape patches in the study area, and the spatial distribution of landscape patches is more uniform.

Shannon Homogeneity Index (SHEI):

$$SHEI = \frac{-\sum_{i=1}^{m}(p_i * \ln p_i)}{\ln m} \tag{8}$$

m is the total number of land use landscape types, and P_i is the percentage of the area of landscape types i that is accounted for by all types of landscapes. When the value of LPI is 0, it indicates that there is no diversity in the landscape system, suggesting that there may be dominant landscape types in the whole landscape system; a value of 1 indicates that the proportion of different landscape patch types in the overall landscape system is the same, and the landscape shows a completely uniform spatial distribution state, indicating that there are no obvious dominant landscape types.

Landscape aggregation index AI:

$$AI = [\frac{g_{ii}}{\max \to g_{ii}}] \times 100 \tag{9}$$

g_{ii} is the number of similar neighboring patches of the corresponding landscape type, and the aggregation index (AI), AI takes values between [0, 100]. AI takes a value of size to reflect the connectivity between patches of various landscape types. The smaller the value, the more discrete the landscape is, and the larger the value, the more concentrated the landscape distribution is.

2.2. SOM-based landscape characterization data for ecosystems

2.2.1. Self-organizing feature mapping networks. Self-organizing feature mapping networks [22-23] (SOM) are also known as Kohonen networks. Self-organizing feature mapping neural networks mimic the self-learning function within the human brain, when the human brain learns from a large amount of information, each neuron is active to a different degree for different information. When the human brain is confronted with different information, different neuronal regions in the brain react differently to different information. For a particular neuron in a particular brain region, it is most sensitive to a particular piece of information. When this information is received the neurons in that area become excited and inhibit other neurons.

2.2.2. Self-organizing feature mapping network structure. Self-organizing feature mapping neural networks learn the features and topology inherent in the input vectors by learning them, and the topological features of this information can be revealed at the output layer. Therefore self-organizing feature mapping neural networks have the ability to advance the pattern features of the input vectors. Generally self-organizing feature mapping neural network includes the following four parts:

1) Unit processing column. Used to accept information input, and these input information to discriminate and calculate the formation of "discriminant function".

2) Comparison and selection mechanism. The discriminant function of the input information of the unit processing column is compared, and the one with the largest function value is selected as the processing unit of the output value.

3) Local interconnection mechanism. Connect neurons to each other by weight vectors, and when an input is obtained, the selected processing neuron and its neighboring neurons are excited.

4) Adaptive process. The sensitivity to a particular input is increased by parameter adjustment of individual neurons (mainly the neurons of the excited processing unit), i.e., by increasing the value of the output of the "discriminant function". This process is generally fine-tuned.

2.2.3. Working principle of self-organizing feature mapping networks. A common feature of biological systems is the ability to derive patterns from their natural environment without a tutor and to follow them. Similarly, this is the goal of self-organizing neural networks: that is, to derive meaningful patterns from input data without supervision. Self-organizing feature mapping neural network is an unsupervised learning algorithm. The neuron structure of the self-organizing feature mapping network is similar to the Hebb neuron of the unsupervised learning rule a Hebb learning rule [24]. The structure of the Hebb neuron is shown in Fig. 1.

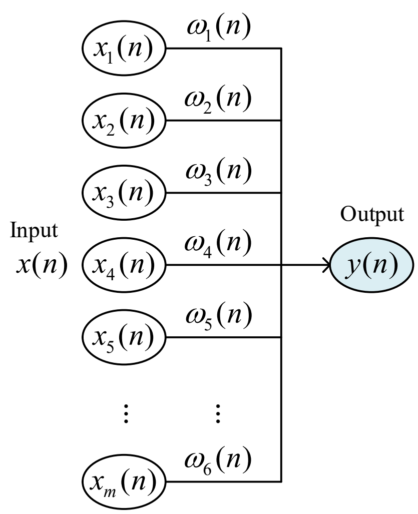

Fig. 1. The structure of the Hebb neuron

It is assumed that when the salient signals of input x and output y coincide, the weights between the two are enhanced, i.e:

$$\omega_i(n+1) = \omega_i(n) + \eta\, y(n) x_i(n) \tag{10}$$

To ensure that the weights do not increase infinitely, each weight is normalized, i.e:

$$\omega_i(n+1) = \frac{\omega_i(n) + \eta\, y(n) x_i(n)}{(\sum(\omega_i(n) + \eta\, y(n) x_i(n))^2)^{1/2}} \tag{11}$$

Thus, for the whole neuron, Assumption $W = [\omega_i]_{xm}, X(n) = \lfloor x_i(n) \rfloor_{1\times m}$, the neuron's weights are adjusted by Eq:

$$W(n+1) = W(n) + \eta\, y(n)(X(n) - y(n)W(n)) \tag{12}$$

In the above equation, the external input $x_i(n)$ is a positive feedback that makes the weights $\omega_i(n)$ increase, while the negative feedback of $-y(n)$ controls the weights $\omega_i(n)$ to decrease, keeping $\omega_i(n)$ stable. The final output is:

$$y(n) = X^T(n)W(n) = W^T(n)X(n) \tag{13}$$

In practice the neuron structure of the self-organizing feature mapping network is Hebb neuron structure, and the learning method uses competitive learning, while strengthening the activated neuron will inhibit the distant neuron, making the neuron more sensitive to specific information.

The self-organizing feature mapping neural network defines a neighborhood function as:

$$h_{j^*,j} = e^{\left(-\frac{\left|r_{j^*}-r_j\right|^2}{2\sigma(t)^2}\right)} \tag{14}$$

where r represents the positions of different neurons $(r \in \Re^2)$, the neighborhood function is defined within a neighborhood range with a radius of σ centered on the winning neuron, and thus this range is called the winning neighborhood. The schematic diagram of the winning domain is shown in Fig. 2.

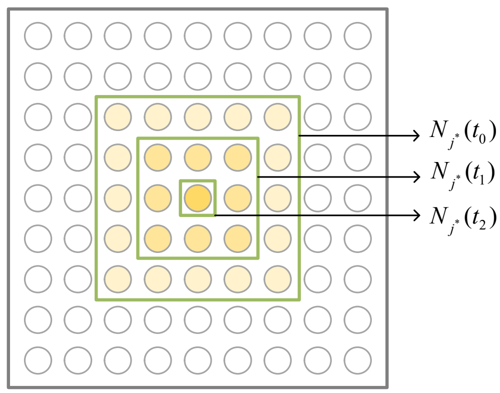

Fig. 2. The winning neighborhood

Assuming that the winning neuron is $i^*, N_{f^*}(\cdot)$ as a function of time t, at the beginning of the learning period, there are more winning neurons at $N_{f'}(t_0)$. The winning neuron and its neighborhood are all close to the input vector at that time, forming a rough mapping. As learning proceeds and decreases, the winning neighborhood becomes narrower, the number of neurons in the vicinity of the winning neuron becomes smaller, the number of winning neurons decreases from $N_{j^r}(t_i)$ to $N_f(t_2)$, and the weight of the neuron gradually increases to eventually reach the predetermined goal of the process.

2.2.4. Algorithmic steps for self-organizing feature mapping networks. Let the input sample set X be a $I \times n$ -dimensional vector containing I samples each of n dimensions, denoted as $X = [x_i]_{|x|}, x_i = [x_{i,1}, x_{i,2}, x_{i,3}, \cdots, x_{i,n}], i = 1,2,3,\ldots,I$. The neural network's weight vector dimension is the same as the dimension of the input layer, so that each neuron has a weight vector of $\omega_j = \left[\omega_{j1}, \omega_{j2}, \omega_{j3}, \cdots, \omega_{jn}\right], j = 1,2,3,\ldots,J$, and J is the number of neurons. The winning neuron is decided by calculating the degree of similarity between the comparison neuron and the weight vector, a common discriminative method is to calculate the distance between the two, generally using the Euclidean distance, i.e.:

$$\|a - b_i\| = \sqrt{(a - b_i)^T (a - b_i)} \tag{15}$$

Or calculate the value of the cosine between the two, i.e:

$$\cos\alpha = \frac{a^r b_i}{\| a \| \| b_i \|} \tag{16}$$

For self-organizing feature mapping neural networks, the most important thing is how to determine the neurons. The specific way is as follows:

1) Normalize the input vector X and the weight vector W of the neurons in the competing layer so that the mode of both is 1;

2) When the network gets an input vector x_i, calculate the Euclidean distance or cosine value between the weight vectors of all neurons in the competing layer and the input, and take the neuron whose weight value is closest to the input vector x_i as the winning neuron. That is, the neuron with the shortest Euclidean distance wins, i.e:

$$O_{j^*} = \arg\min_{j\in\{1,2,3,\cdots,J\}} \left\| x_j - \omega_j \right\| \tag{17}$$

Since after normalization the maximum similarity is the maximum inner product, ie:

$$O_{j^*} = \max_{je\{1,2,3,\cdots,J\}} (\tilde{W}_j^{T} \tilde{X}) \tag{18}$$

After finding the winning neuron mark the winning neuron as 1 and the non-winning neuron as 0, i.e:

$$O_j(t+1) = \begin{cases} 1 & j = j^* \\ 0 & j \neq j^* \end{cases} \tag{19}$$

At the same time the weights of the neurons are adjusted, i.e:

$$\begin{cases} \omega_j(t+1) = \omega_j(t) + \Delta\omega_j(t) & j = j^* \\ \omega_j(t+1) = \omega_j(t) & j \neq j^* \end{cases} \tag{20}$$

When the winning neuron and its neighboring neurons are updated, another input vector goes into training to find the best neuron. Until the algorithm stops after the network has learned all the inputs and outputs the final result.

In summary, the steps of the algorithm for self-organizing feature mapping neural network are:

1) Initialization of the network: determine the structure of the network, the number of neurons, the weight vector is assigned an initial value, the learning rate of the network is determined $\eta(t)$, and the initial values of the neighborhood function $h_{(i,j)}(t)$, $\eta(t_0)$ and $h_{(i,j)}(t_0)$.

2) For the input vector and the initialized weights of the network are normalized, the normalization formula is:

$$\begin{cases} \overline{x}_i = \dfrac{x_i}{\| x_i \|} \\ \overline{\omega}_i = \dfrac{\omega_i}{\| \omega_i \|} \end{cases} \tag{21}$$

3) Neuron competition to select the winning neuron. Referring to Eq. (15) or (16), the Euclidean distance or cosine value is calculated and the smallest one is selected as the winning neuron. At the same time, in order to make the network with clustering function for the winning neuron to define a topological domain N_{j^*}, so that the output inside N_{j^*} is 1, and the output outside N_{j^*} is 0, that is:

$$\begin{cases} y_i = 1, i \in N_C \\ y_i = 0, i \notin N_C \end{cases} \tag{22}$$

4) Updating the weights: the formula for updating the weight vector after referring to Eq. (20) can be expressed as:

$$\begin{cases} \omega_j(t+1) = \omega_j(t) + \eta(t) h_{j^*,j}(t) \left\| x_i(t) - \omega_j(t) \right\| & j = j^* \\ \omega_j(t+1) = \omega_j(t) & j \neq j^* \end{cases} \tag{23}$$

5) Update the learning rate $\eta(t)$ and neighborhood function $h_{(i,j)}(t)$.

6) Through the learning, determine whether to meet the set stopping conditions, if it meets, stop and go to the next step, if it does not meet, go to step (2) to train from new.

7) Marking. If the pre-set stopping condition is satisfied, label each best neuron, a neuron corresponds to a class of sample labels.

The self-organizing feature mapping neural network training process is shown in Fig. 3.

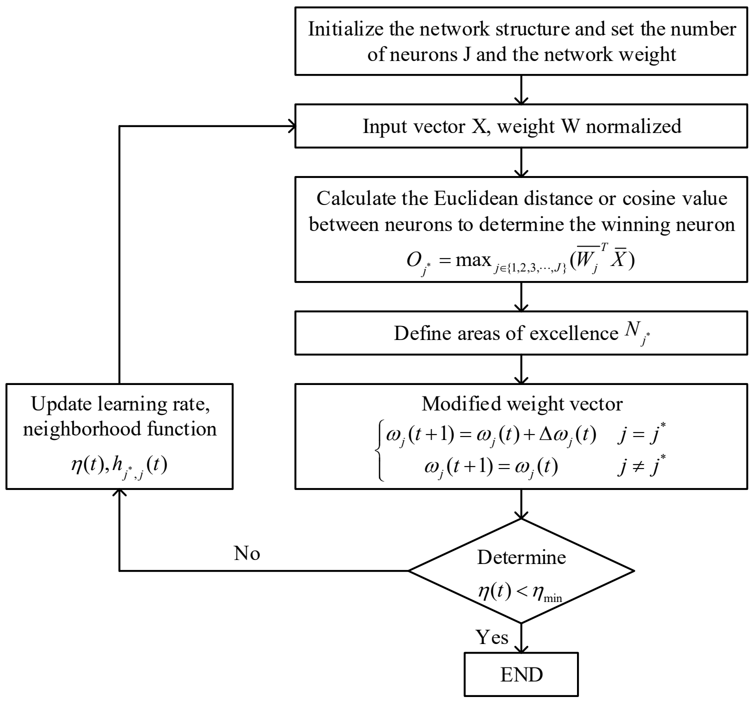

Fig. 3. Training flowchart of self-organizing feature mapping neural network

3. Ecological landscape characterization data and analysis

3.1. Characterization of changes in ecological landscape patterns

The study uses Site A as an example for data characterization of ecological landscape patterns and SOM.

3.1.1. Moving window method window selection. When using the moving window method to calculate the landscape index, the choice of the window scale will have an impact on the results of the landscape index: a smaller window scale may not be able to reflect the internal variability of the landscape, and a larger window scale may lead to the loss of the spatial information of the landscape index. In order to determine the appropriate window size in the moving window method, this study calculates the landscape indices under seven window scales: 1000m, 2000m, 3000m, 4000m, 5000m, 6000m, and 7000m, and determines the appropriate window size by comparing the changes of the landscape indices under different scales. The window size was determined by comparing the changes of landscape indices under different scales. The results of landscape indices at different window scales are shown in Fig. 4. a~h represent patch density, average patch area, edge density, area-weighted average morphology index, aggregation, spreading, Shannon diversity index, and Shannon uniformity index, respectively.

The figure shows the variation of patch density (PD), average patch area (AREA-MN), edge density (ED), area-weighted average shape index (SHAPE-AM), aggregation index (AI), spreading index (CONTAG), shannon diversity index (SHDI), and shannon homogeneity index (SHEI) at different window scales. Among them, the mean values of PD and AI decreased with the increase of the window scale and finally stabilized, specifically, they were unstable at the scales of 1000m and 2000m, and the mean values decreased with the increase of the window scale, and the decrease started from 3000m, and then stabilized at about 4000m, and the distribution of the data from 5000m to 7000m almost did not change anymore, but the anomalous values of PD increased. AREA-MN, ED, CONTAG and SHDI gradually decrease and finally stabilize with the increase of window scale, which shows that the increase of mean value changes drastically in 1000m and 2000m scale, and then decreases significantly in 3000m scale, and there are fewer anomalies and decrease in the change of 4000m scale, and 5000m-7000m data tends to be stable but with more anomalous values. The mean value of SHAPE-AM increased gradually with the increase of the window, while the SHEI showed an increase and then a decrease, neither of which showed an obvious regularity. Therefore, considering the stability of the landscape index, the spatial resolution of the land use data, and the scope of the study area, as well as combining with previous studies, we chose 4000m as the window scale for calculating the landscape index, in order to analyze the characteristics of the changes in the landscape pattern in the eastern part of H province.

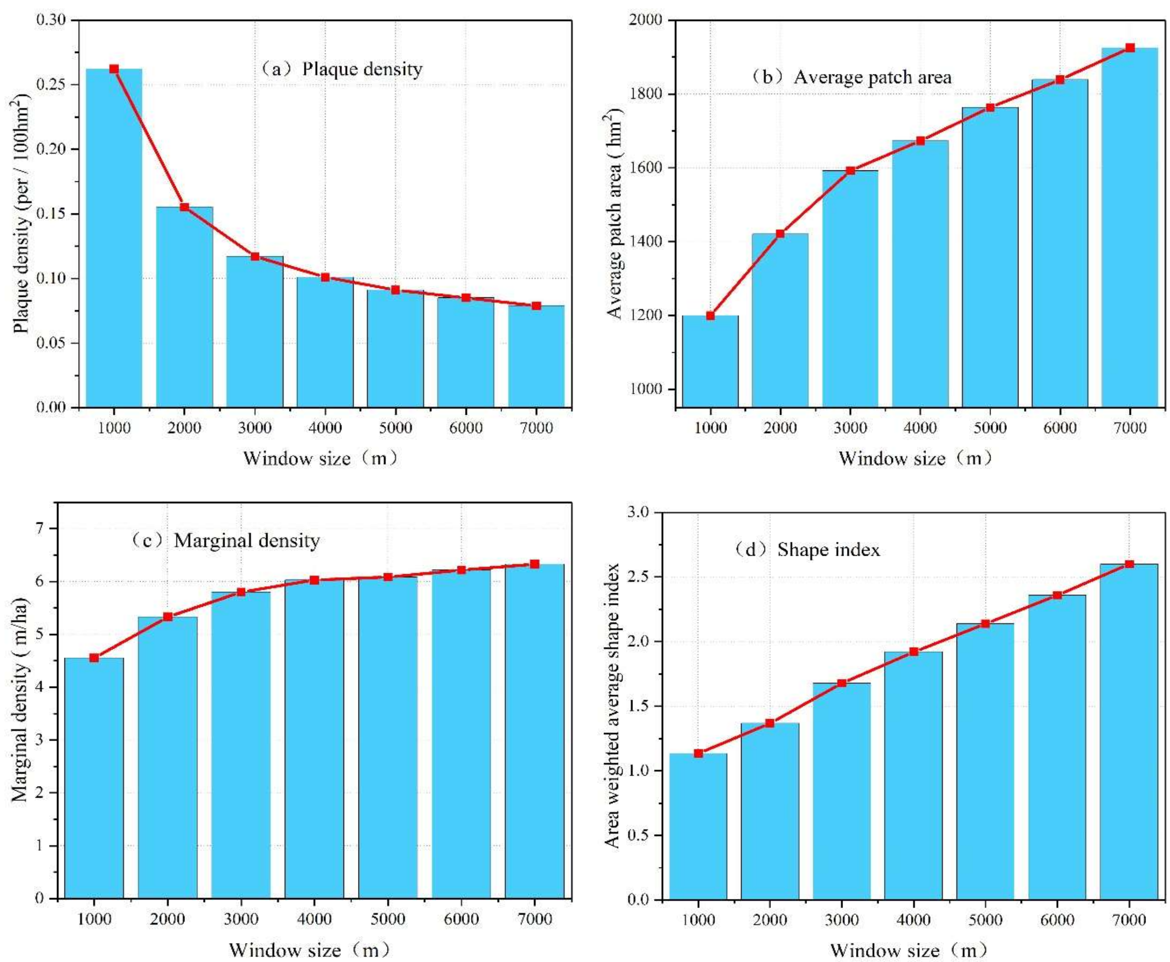

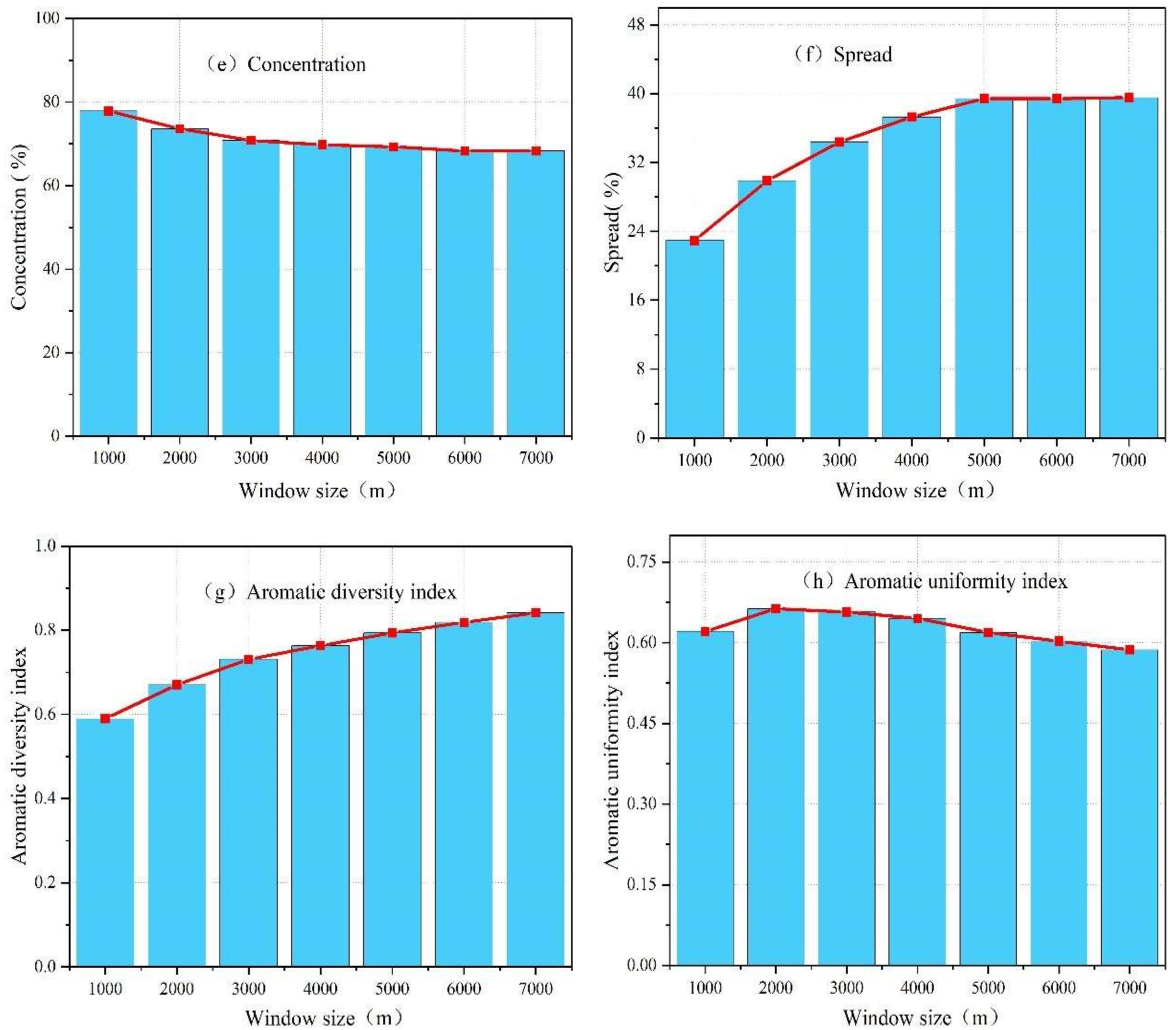

Fig. 4. The results of the landscape index in different window scales

3.1.2. Characteristics of changes in the landscape level index. Landscape indices highly condense the information of landscape pattern, which is a simple quantitative index reflecting the characteristics of its structural combination and spatial configuration, and different types of landscape indices reflect the changing characteristics of landscape structure. We selected eight indices, including PD, AREA-MN, ED, SHAPE-AM, AI, CONTAG, SHDI and SHEI, at the 4000 m window scale to more comprehensively represent the spatial and temporal change characteristics of the landscape pattern in the eastern part of Province H in terms of the degree of landscape fragmentation, the complexity of landscape shapes, the landscape agglomeration, the landscape connectivity and the landscape diversity, etc. The changes of landscape level indices in the eastern part of Province H from 2010 to 2020 are shown in Table 1. The changes of landscape level index in the eastern part of Province H from 2010 to 2020 are shown in Table 1. As can be seen from the table, except for AREA-MN, AI and CONTAG, which are increasing, the rest of the indices show a decreasing trend.

Table 1. The eastern landscape level of h province in 2010—2020

Landscape index	2000	2010	2015	2020	2020
PD	0.0972	0.0973	0.0978	0.0983	0.0914
AREA-MN	1476.0003	1473.9981	1470.0007	1467.0019	1655.0011
ED	6.1969	6.1845	6.2505	6.3072	5.7642
SHAPE-AM	1.9053	1.9032	1.9031	1.9025	1.8614

AI	69.8962	69.9069	68.8777	69.7866	73.945
CONTAG	34.9395	34.9588	34.9682	34.8093	37.9551
SHDI	0.7271	0.7279	0.7284	0.7109	0.6922
SHEI	0.6394	0.6392	0.6491	0.6497	0.6199

3.1.3. Analysis of changes in type level indices. Six landscape indices such as aggregation index (AI), average patch area (AREA-MN), edge density (ED), patch density (PD), area-weighted average shape index (SHAPE-AM), and combination index (COHESION) were selected at the type level to explore the 1cropland, 2forest, 3grassland, from the perspectives of landscape fragmentation, shape complexity and connectivity, 4 waters, 5 construction land and 6 unutilized land landscape type change characteristics, and the change characteristics of the type level index in the eastern part of Province H from 2010 to 2020 are shown in Figure 5. A~f represent aggregation index (AI), average patch area (AREA-MN), edge density (ED), patch density (PD), area-weighted average shape index (SHAPE-AM), and binding index (COHESION), respectively. Between 2010 and 2020, AI, AREA-MN, and COHESION were in an increasing trend, while ED, PD, and SHAPE-AM were in a decreasing trend, suggesting that there is an increase in aggregation and connectivity within the landscape types in the study area, but that the shape of the patches is becoming more complex. The level of aggregation varies greatly among landscape types, with woodland being the lowest at 59.34%, watershed being the highest, far exceeding the other types at more than 88.77%, and the rest of the types being grassland, unutilized land, cropland, and built-up land in descending order of aggregation.

The largest increase in aggregation was in grassland at 3.09%, which is related to the conversion of unutilized land to grassland in the southwestern part of the study area. Cultivated land patches have the second largest increase in aggregation after grassland, with 2.56%, which indicates that cultivated land tends to be more aggregated than other types of landscapes, which is convenient for human beings to concentrate on activities related to production and life. The increase in aggregation of construction land was higher than that of unutilized land, forest land and water, which, together with the change in aggregation of cultivated land, indicated that human activities such as urban construction and food cultivation also tended to be aggregated in the study area.

The landscape type with the largest average patch area is water, which is about 4456.45 hm^2, which is about the same as the area of Lake H in the study area, and the highest degree of aggregation is also in water, both of which indicate that water landscapes in the study area mainly consist of a small number of patches with large areas aggregated together. Built-up land and cropland were at the lower end of the range for each type, suggesting that human activities have resulted in a more fragmented landscape. The largest increase in average patch area is grassland the smallest increase is unutilized land, the ecological recovery of grassland vegetation in the study area is obvious under the implementation of engineering measures such as returning pasture to grassland, fencing and grazing ban. The edge density and area-weighted average shape index of woodland landscape were the highest among all types, indicating that the shape of woodland landscape in the study area was more complex, and at the same time, woodland was the only type in the study area that showed an increase in the complexity of landscape shape.

Forested land in the study area is mainly located in areas with better hydrothermal conditions and higher elevations, with a large area and a fine belt distribution, resulting in a more fragmented forested landscape than other types, which increases the difficulty of protection and management, and is also intertwined with cropland, grassland, and unutilized land, which are unevenly distributed.

The landscape complexity of cultivated land and construction land is also in the higher category, indicating that human development often contributes to the complexity of landscape shapes. The patch density of each landscape type showed a trend of increasing and then decreasing, and the landscape type with the highest density was construction land, about $0.1499/hm^2$, and the lowest was water about $0.053/hm^2$, indicating that the construction land had the highest degree of fragmentation.

The decrease of patch density and the increase of average patch area imply that the aggregation of various types of landscapes in the study area has increased and become more concentrated, indicating that the influence of human activities on the overall landscape structure and function of the study area is gradually increasing. The conversion of large areas of unutilized land to grassland resulted in grassland being the landscape with the highest reduction in patch density after cropland, and also the most connected landscape except for water.

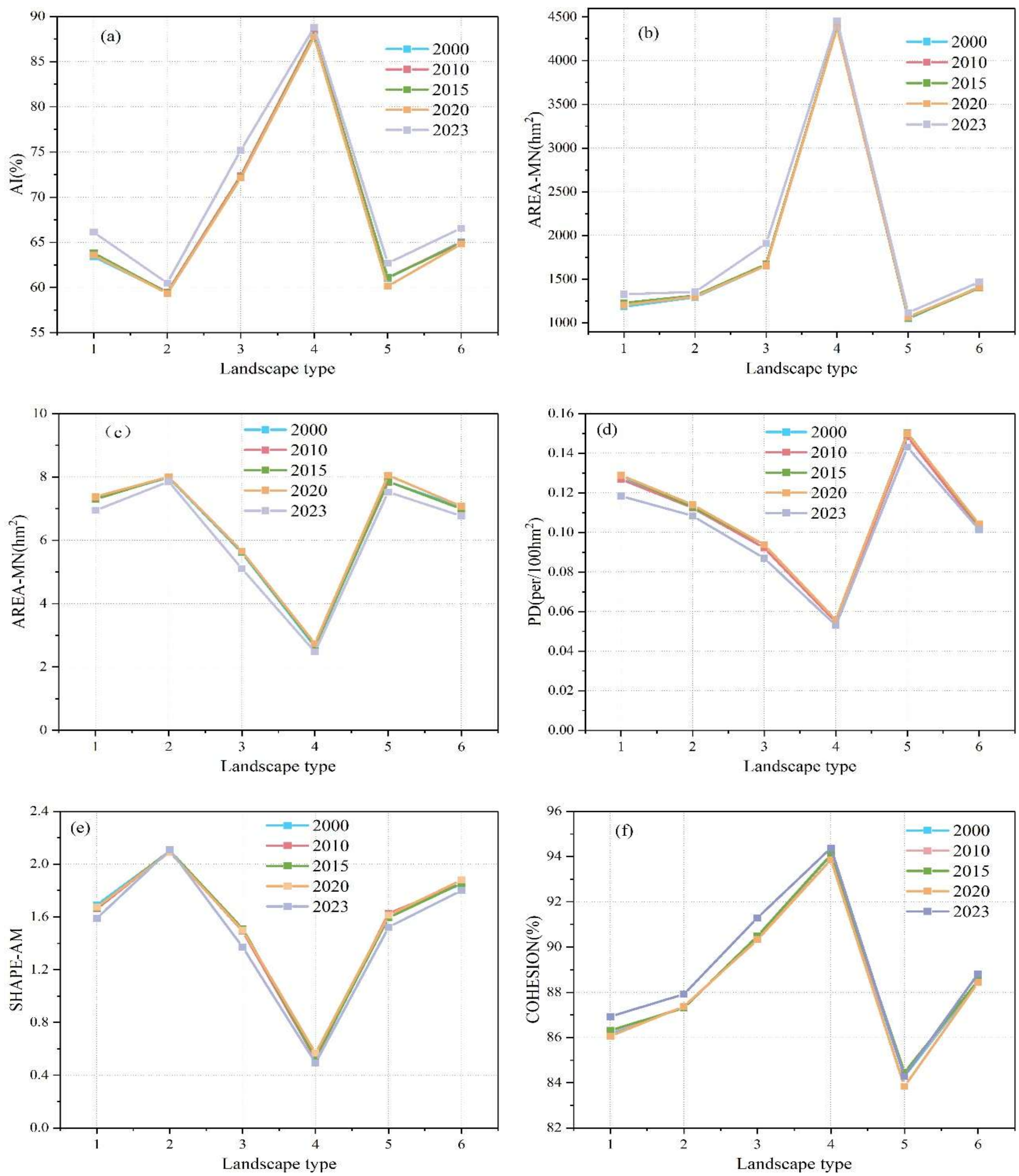

Fig. 5. The eastern type horizontal index changes in h province

3.2. *Ecological landscape characterization data results*

In this study, the network model takes different number of clusters sequentially, which can get different clustering results. The land landscape types utilized in this paper are 1 Cultivated land, 2 Forest land, 3 Grassland, 4 Watershed, and 5 Construction land. The training step size affects the accuracy of classification, and 1000, 2000, 3000, 4000 and 5000 trials were conducted in this study. The results of the clustering pattern distribution are shown in Figure 6, with a~c representing the number of clusters from 2 to 4, respectively. As can be seen from the clustering pattern distribution graph, the clustering results are different for different numbers of output neurons. When the number of output neurons is small (S=2 and 3), the land use landscape changes of various clustering patterns are not significant. When the number of output neurons is higher, there is a clustering vacancy, but the changes of various clustering patterns become very obvious and the clusters are finer. It can be seen that the more the number of output neurons, the finer the effect of clustering and the more significant the changes.

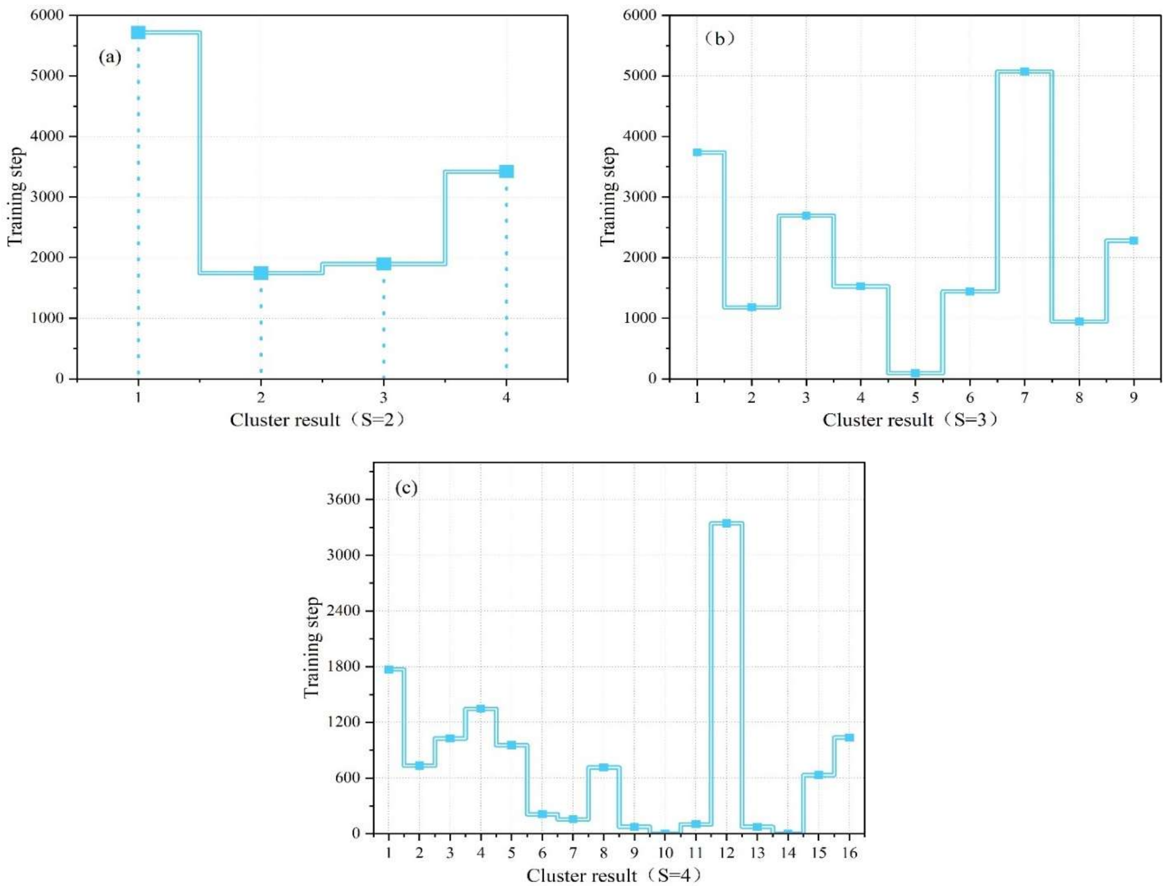

Fig. 6. Cluster pattern distribution results

4. Conclusion

In order to realize the landscape characterization data of ecological environment, this paper proposes the self-organized feature mapping network (SOM) and constructs the data characterization model with self-learning function to obtain the law of ecological environment landscape change. The comparison results of the moving window method show that the landscape index is unstable in the 1000-3000m window, the magnitude of change begins to decrease in the 4000m scale, the data distribution tends to be stable and has fewer outliers in the 5000m scale, and the data is more stable but has more outliers in the 6000-7000 scale. The PD, ED, SHAPE-AM, SHDI, and SHEI indices all show decreasing trends, except for AREA-MN, AI, and CONTAG, which are increasing. At the landscape level, patch density, edge density, area-weighted mean shape index, Shannon diversity index, and Shannon evenness index showed decreasing trends, except for the mean patch area, aggregation index, and spread index, which indicated that the overall landscape aggregation and connectivity in the study area was increasing, and landscape fragmentation, complexity, and diversity were decreasing.

References

[1] Laurila-Pant, M., Lehikoinen, A., Uusitalo, L., & Venesjärvi, R. (2015). How to value biodiversity in environmental management?. Ecological indicators, 55, 1-11.

[2] Goss, R., & Lepetit, B. (2015). Biodiversity of NPQ. Journal of plant physiology, 172, 13-32.

[3] Ulanowicz, R. E. (2020). Quantifying sustainable balance in ecosystem configurations. Current Research in Environmental Sustainability, 1, 1-6.

[4] Chen, W., Chi, G., & Li, J. (2020). The spatial aspect of ecosystem services balance and its determinants. Land Use Policy, 90, 104263.

[5] Shapiro, J., & Báldi, A. (2014). Accurate accounting: How to balance ecosystem services and disservices. Ecosystem Services, 7(0), 201-202.

[6] Tsujimoto, M., Kajikawa, Y., Tomita, J., & Matsumoto, Y. (2018). A review of the ecosystem concept—Towards coherent ecosystem design. Technological forecasting and social change, 136, 49-58.

[7] Himeur, Y., Rimal, B., Tiwary, A., & Amira, A. (2022). Using artificial intelligence and data fusion for environmental monitoring: A review and future perspectives. Information Fusion, 86, 44-75.

[8] Pattyam, S. P. (2021). AI-Driven Data Science for Environmental Monitoring: Techniques for Data Collection, Analysis, and Predictive Modeling. Australian Journal of Machine Learning Research & Applications, 1(1), 132-169.

[9] Wani, A. K., Rahayu, F., Ben Amor, I., Quadir, M., Murianingrum, M., Parnidi, P., ... & Latifah, E. (2024). Environmental resilience through artificial intelligence: innovations in monitoring and management. Environmental Science and Pollution Research, 31(12), 18379-18395.

[10] Zhang, X., Shu, K., Rajkumar, S. A., & Sivakumar, V. (2021). Research on deep integration of application of artificial intelligence in environmental monitoring system and real economy. Environmental Impact Assessment Review, 86, 106499.

[11] Shaikh, R. A. J., Naidu, H., & Kokate, P. A. (2021). Next-generation wsn for environmental monitoring employing big data analytics, machine learning and artificial intelligence. In Evolutionary Computing and Mobile Sustainable Networks: Proceedings of ICECMSN 2020 (pp. 181-196). Springer Singapore.

[12] Popescu, S. M., Mansoor, S., Wani, O. A., Kumar, S. S., Sharma, V., Sharma, A., ... & Chung, Y. S. (2024). Artificial intelligence and IoT driven technologies for environmental pollution monitoring and management. Frontiers in Environmental Science, 12, 1336088.

[13] Podorozhniak, A., Liubchenko, N., Kvochka, M., & Suarez, I. (2021). Usage of intelligent methods for multispectral data processing in the field of environmental monitoring. Advanced Information Systems, 5(3), 97-102.

[14] Asha, P., Natrayan, L. B. T. J. R. R. G. S., Geetha, B. T., Beulah, J. R., Sumathy, R., Varalakshmi, G., & Neelakandan, S. (2022). IoT enabled environmental toxicology for air pollution monitoring using AI techniques. Environmental research, 205, 112574.

[15] Krupnova, T. G., Rakova, O. V., Bondarenko, K. A., & Tretyakova, V. D. (2022). Environmental justice and the use of artificial intelligence in urban air pollution monitoring. Big Data and Cognitive Computing, 6(3), 75.

[16] Xu, K. (2023). Artificial intelligence unlocks ecological environment governance—smart statistical monitoring based on meteorology. Multimedia Tools and Applications, 82(14), 21613-21625.

[17] Mishra, A., & Priyadarshini, R. (2022). Environmental monitoring in wireless sensor networks using AI. In Artificial Intelligence (pp. 71-102). Chapman and Hall/CRC.

[18] ANDREI, N., & IOANID, A. (2023, December). Potential use of artificial intelligence and geospatial analysis in environmental monitoring: Air quality in a large city. In International Conference of Management and Industrial Engineering (Vol. 11, pp. 369-376).

[19] Karthika, D. (2023). A study on artificial intelligence for monitoring smart environments. Materials Today: Proceedings, 80, 2009-2013.

[20] Ullo, S. L., & Sinha, G. R. (2020). Advances in smart environment monitoring systems using IoT and sensors. Sensors, 20(11), 3113.

[21] Nazarov, D., Sulimin, V., & Shvedov, V. (2024). Advancing environmental stewardship: The role of automation in enhanced environmental monitoring. In E3S Web of Conferences (Vol. 542, p. 05005). EDP Sciences.

[22] Yi Zeng Hsieh ,Chia Hsuan Wu& Yu Ting Chen. (2024). Integrating self-organizing feature map with graph convolutional network for enhanced superpixel segmentation and feature extraction in non-Euclidean data structure. Multimedia Tools and Applications(prepublish),1-26.

[23] Liu Li,Hua Chi,Cheng Zixuan & Ji Yunfeng. (2021). Intelligent Diagnosis Method of MRI Brain Image Using Parallel Self-Organizing Feature Maps Neural Network. Journal of Medical Imaging and Health Informatics(2),487-496.

[24] Cristian Napole,Oscar Barambones,Isidro Calvo & Javier Velasco. (2020). Feedforward Compensation Analysis of Piezoelectric Actuators Using Artificial Neural Networks with Conventional PID Controller and Single-Neuron PID Based on Hebb Learning Rules. figurEnergies(15).